# CHAPTER XII

# IMPACT-DETECTION EXPERIMENT

By Alfred G. Beswick
Langley Research Center

## SECTION I - INTRODUCTION

A meteoroid-particle impact-detection experiment was included as one of the secondary experiments of the Explorer XIII satellite. Its main purpose was to extend micrometeoroid measurements to a low population range where few data exist. An additional purpose was to correlate with and to augment the data amassed by previous satellites employing similar experimental technique. Impact detectors having three threshold levels of momentum sensitivity, nominally 0.01, 0.1, and 1.0 gram-centimeter per second, were provided to meet these objectives.

An impact detector consists of an impact-sensitive detecting surface with an attached transducer, and signal-conditioning, impact-event counting, and count-storage circuitry. Two physical configurations of detecting surface were used. One configuration was a pair of stainless-steel plates having total geometric area of 0.142 square meter mounted on the conical portion of the satellite forward shell and used for the high and the low sensitivity impact detection. The twenty 0.005-inch-thick pressurized-cell penetration detectors were also sensitized for impact detection and formed the second type of detecting surface. This configuration had a detecting surface area taken as 0.186 square meter and was used for intermediate sensitivity impact detection.

## SECTION II - IMPACT-DETECTION-SYSTEMS OPERATION

The operation of the meteoroid-impact-detection systems depended upon the development of a propagating mechanical perturbance due to meteoroid particle impact upon a detecting surface. Figure XII-1 is a block diagram of the elements of the pressurized-cell impact-detection system, and figure XII-2 is a block diagram of the elements of the curved-plate system. The figures indicate the manner in which the transducer elements of the detecting surfaces were arrayed. The operations and functional elements of both systems are essentially the same. As indicated by figures XII-1 and XII-2, particle impact upon a detecting surface produces a propagating mechanical perturbance which is transduced to a representative electrical signal by the piezoelectric element attached to the underside of the surface. Figure XII-3 shows oscilloscope photographs of typical calibration impact signals. The transducer impact signal is routed to signal-conditioning circuitry and then to impact-event counting and count-storage circuitry.

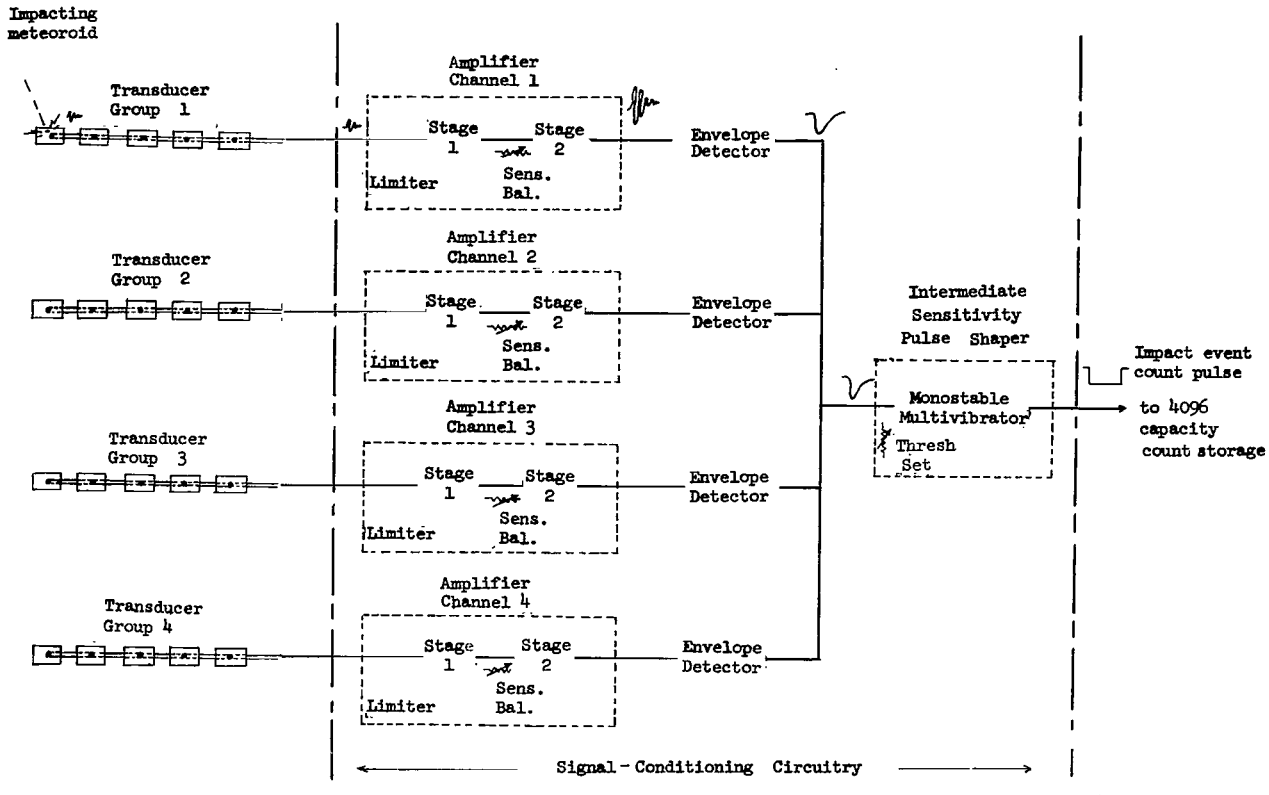


Figure XII-1.- Block diagram of pressurized-cell impact detection system.

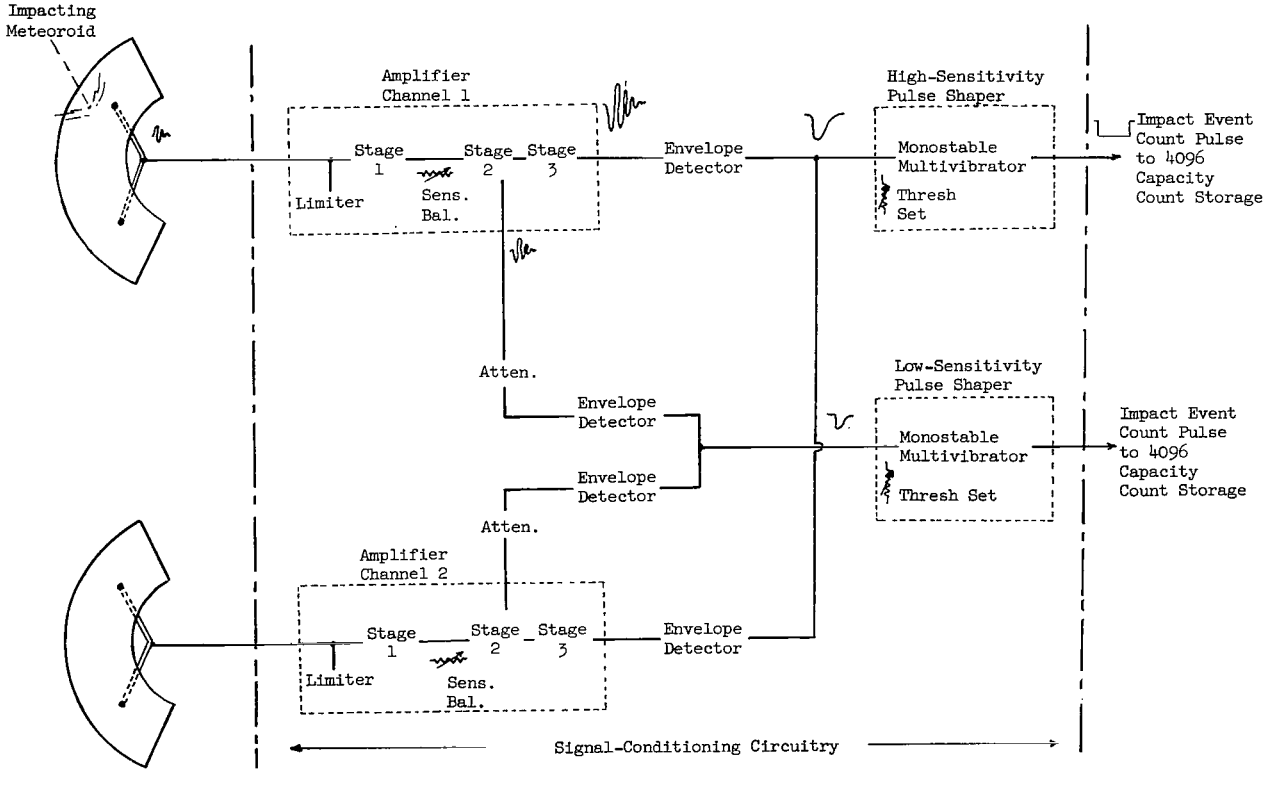


Figure XII-2.- Block diagram of curved-plate impact detection system.

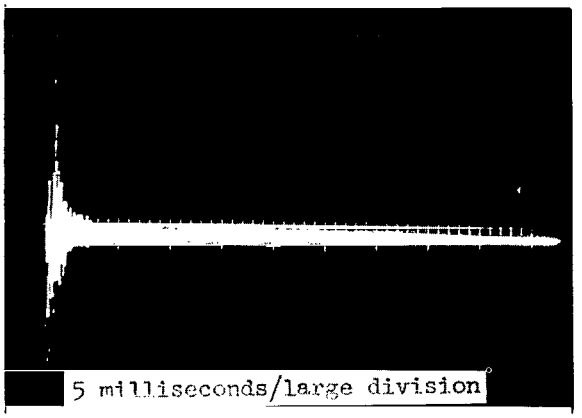


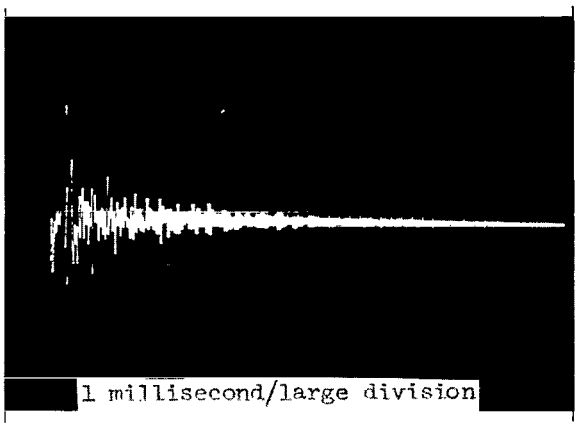


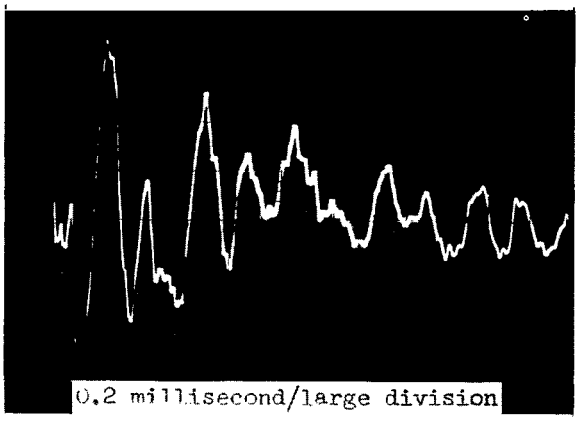


Figure XII-3.- Oscilloscope photographs of typical calibration impact signals.

The impact-detection-signal conditioning circuitry consists of a broadband amplifier and envelope detector, interconnection circuitry and a monostable multivibrator pulse shaper. Each transducer array has a separate amplifier and envelope detector channel.

The amplifier increased the transducer signal amplitude by a factor depending upon the required detection sensitivity. After amplification, the signal was applied to the envelope detector where it was rectified, and its high-frequency components filtered out. The impact signal at this point was then a replica of the negative half of the envelope of the signal originally developed by the piezoelectric element. The envelope detectors of each amplifier channel were paralleled by interconnection on their output side. Thus, a signal from any of the transducers of a given detecting-surface array could be treated by just one pulse-shaping circuit.

The signal was then applied to the input of the monostable multivibrator pulse-shaper circuit, the voltage bias level of which, in combination with the signal amplification factor, defined the detection-sensitivity threshold; sufficiently large signal amplitudes triggered the multivibrator which then executed its cyclic excursion; signal amplitudes below threshold level were not recognized.

The output signal of the multivibrator pulse-shaper circuit was the impact-event counting pulse. Its constant parameters provide a better form of input signal for the counting and storing circuitries than the originally transduced impact signal. The status of the impact event-counting and storage circuitries was telemetered whenever the satellite

transmitted its data. Thus, the number of impacts accumulated between data transmissions could be determined from the received data. Details of the circuitries which accomplished the impact event counting and count storage will be found in chapter IV of this compilation.

## SECTION III - DESCRIPTION OF INSTRUMENTATION

Description of the instrumentation of the meteoroid-impact-detection experiment is divided into three parts: the impact-detecting surface arrays and their attached transducers, the associated electronic signal-conditioning circuitries, and the impact event-counting and count-storage circuitries.

Detecting Surfaces and Transducers.- The impact-sensitized detecting surfaces were arrayed in two forms. Figure XII-4 is a photograph of the stainless-steel curved-plate detecting surfaces showing the location of a pair of electrically paralleled transducer assemblies on the undersurface. These detecting surfaces were fixed to the satellite forward shell by raised acoustic isolator stand-offs. Figure XII-5 is a photograph of one of the pressurized-cell

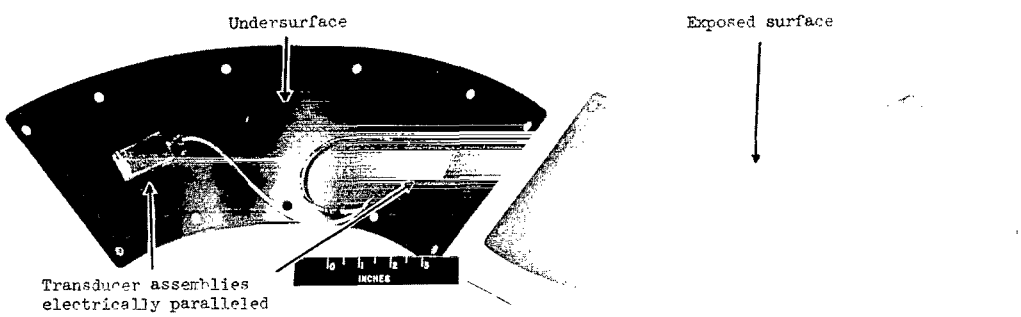


L-62-8817.1

Figure XII-4.- Stainless-steel curved-plate detecting surfaces.

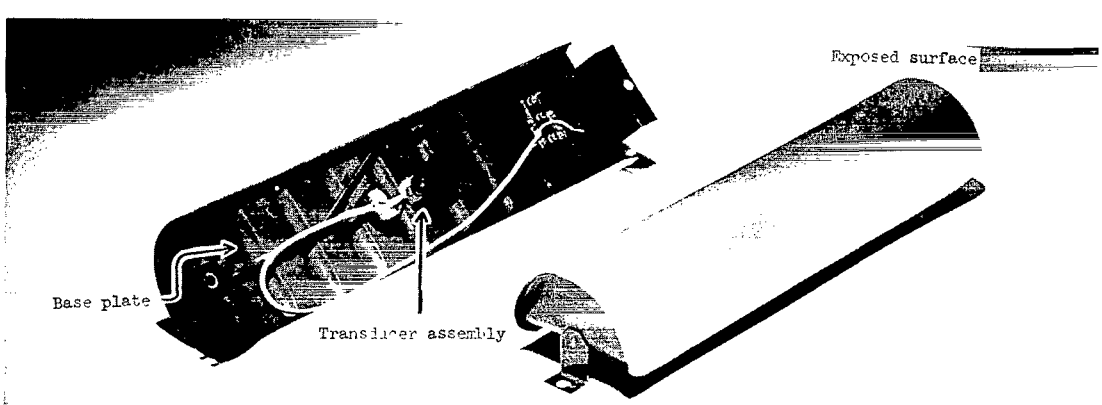


Figure XII-5.- Impact-sensitized pressurized cell. L-64-1980.1

detectors showing the location of the impact sensitizing transducer assembly on its base plate. The 20 impact sensitized pressurized-cell detectors were distributed on the satellite periphery as shown schematically in figure IV-22. Table XII-I lists the pertinent physical parameters of the two configurations of detecting surfaces.

The impact-sensitizing transducer assembly was the same for both types of detecting surfaces. Figure XII-6 is a drawing of the components of the assembly. The sensitive element of the transducer assembly was the lead-zirconate titanate piezoelectric disk, part 4 of figure XII-6. This element was operated in a prestressed thickness expander mode, and the electrical signal resulting from particle impact was taken across the disk flats by the electrodes, part 7. The static loading was supplied by the cantilever spring, part 1, which also had the function of holding the assembly in place. The fused quartz transfer disk, part 5, coupled the impact perturbation signal to the piezoelectric disk, while maintaining electrical isolation from the satellite structure. The insulator disk, part 3, preserved electrical isolation and also served as a spacer. The transducer assembly was keyed in place by the dimple in the cantilever spring tip, which rested in the depression on the top of the domed brass locating disk, part 2. The thickness of part 2 was varied to adjust the static loading on the piezoelectric element to a desired value for each assembly. The assembly was prevented from gross lateral movement by the diallyl-phthalate holding collar, part 6, which had a slot for leadout of the electrodes. The curved-plate detecting surface transducer assemblies were covered by an electrical interference shield and dust cover.

Tests showed that the transducer assemblies could be operated in electrically paralleled groups without significant detriment. Thus, the transducers of the 20 pressurized-cell detectors were interconnected in groups of five cells each. Each curved-plate detecting surface employed an electrically paralleled pair of transducers in order to improve its response uniformity.

Signal-Conditioning Circuitries.- The impact signals from the detecting surface transducers are sharply damping oscillations (fig. XII-3), and their predominant frequency components range from 5 to 40 kilocycles. Such signals required conditioning to become compatible with the data storage and telemetry systems of the satellite. The signal-conditioning circuitry consists of a broadband amplifier, an envelope detector, and a pulse shaper. Since the signal-conditioning circuitries are continuously powered in orbit, a minimum power-consumption design was required.

Each of the two detecting surface configurations has its signal-conditioning circuitry constructed in a separate modular package. Thus, there are four amplifier channels and envelope detectors in the impact-sensitized pressurized-cell signal-conditioning circuitry module, and two amplifier channels in the curved-plate detecting-surface signal-conditioning circuitry module. Figures XII-7 and XII-8 are photographs of the pressurized-cell and curved-plate signal-conditioning-circuitry modules, respectively.

Figure XII-9 is a schematic diagram of the signal-conditioning circuitry of the impact-sensitized pressurized-cell detectors. The four amplifier and envelope detector channels associated with the four transducer groups are shown

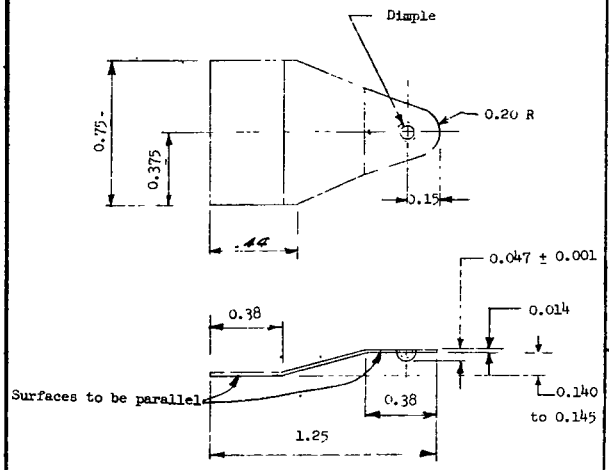


Part 1.- Holding clamp

Scale- 2:1

Material- Beryllium copper deoxidized after heat treatment

Heat treatment- Heat to 600° F and hold for 3 hours.

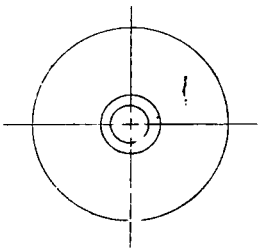

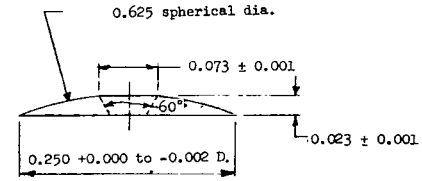


Part 2.- Dome

Scale- 8:1

Material- Brass

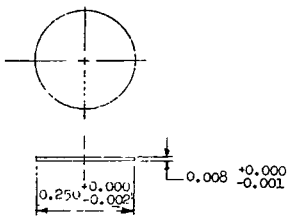


Part 3.- Insulator spacer

Scale- 4:1

Material- Ruby mica

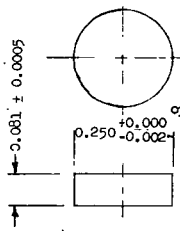


Part 4.- Piezoelectric element

Scale- 4:1

Material- Lead zirconate titanate

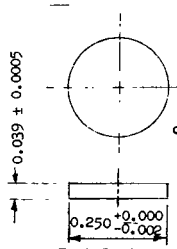


Part 5.- Transfer disk

Scale- 4:1

Material- Fused quartz

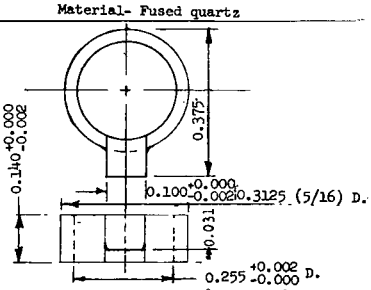


Part 6.- Holding collar

Scale- 4:1

Material diallyl-phthalate

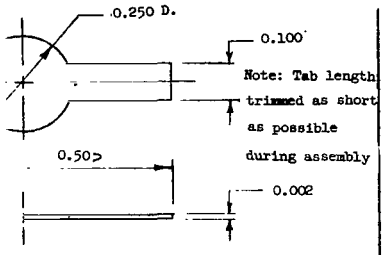


Part 7.- Contact electrode

Scale- 4:1

Material- 0.002 in. gold-plated copper foil

| Part | No. req'd | Part description |
|---|---|---|
| 1 | 1 | Holding clamp |
| 2 | 1 | Dome |
| 3 | 1 | Insulator spacer, mica |
| 4 | 1 | Piezoelectric element |
| 5 | 1 | Transfer disc |
| 6 | 1 | Holding collar |
| 7 | 2 | Contact electrode |

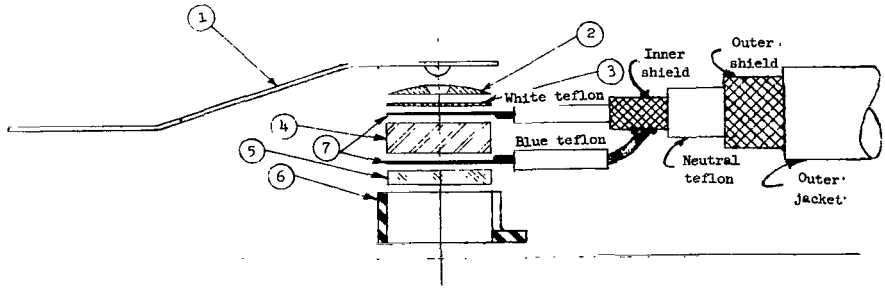


Assembly of

micrometeoroid impact detector crystal stack

Scale - 4:1

Note: Jacket coaxial cable (or single shielded) optionally used (low sensitivity requirements)

Figure XII-6.- Impactor detector transducer detail and assembly.

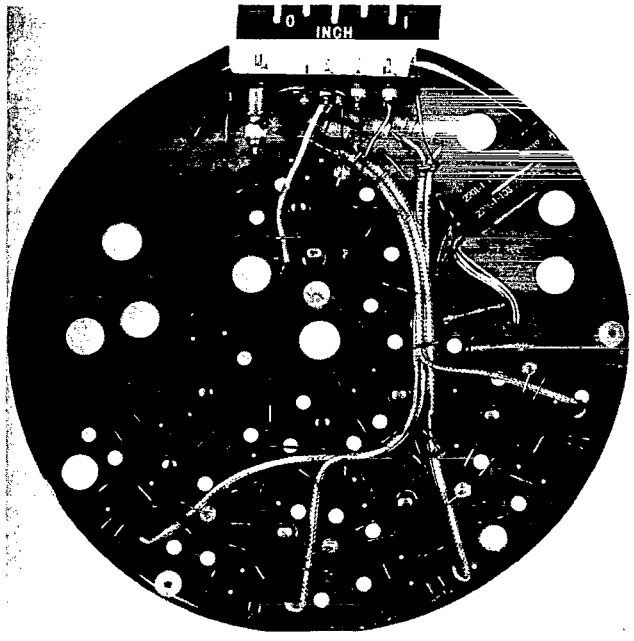


L-61-2022

Figure XII-7.- Signal-conditioning circuitry module for impact-sensitized pressurized cells.

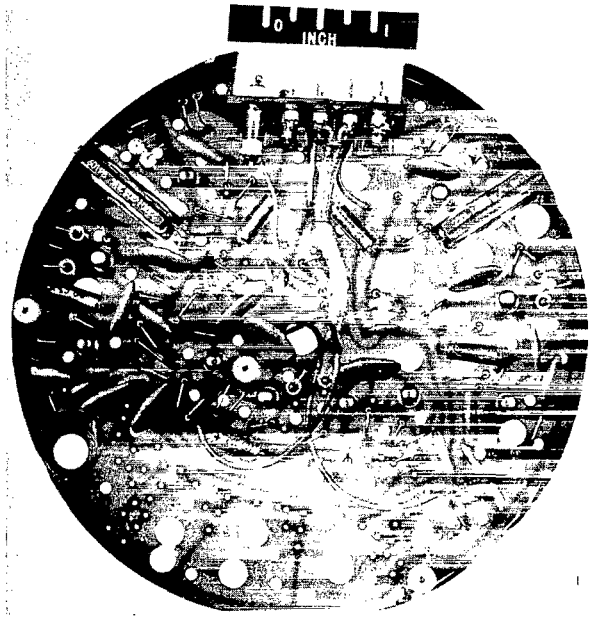


L-61-2023

Figure XII-8.- Signal-conditioning circuitry module for curved-plate impact detecting system.

in figure XII-9. The input to the amplifier portion of each channel has a low pass filter to exclude radio-frequency signals and a shunt-diode limiter to prevent excessive transducer signals from possibly damaging the input transistor. The two amplifier stages are operated at fixed bias voltages, by-passed emitters, and very low quiescent collector currents. Equalization of transducer signal amplitude is provided by a variable resistance in the second amplifier stage. The amplifier section has a voltage amplification factor of about 900:1. Frequency-response and gain-linearity characteristics for this amplifier are shown in figures XII-10 and XII-11, respectively. A double-diode half-wave rectifier and shunt capacitor is used as an envelope detector to rectify and smooth the amplified signal at the output of each amplifier channel. The outputs of the four channels are interconnected following the envelope detectors, and signals from each channel are thus applied to the monostable multivibrator pulse shaper. The multivibrator will only respond to signals having amplitudes equal to or greater than the bias voltage level at its input, thus, a sensitivity threshold is established. When it is triggered, the multivibrator pulse shaper generates a signal of constant duration and amplitude, which has a short rise time. The duration of the multivibrator cycle is sufficient to prevent it triggering more than once by a single impact event. The constant parameters of the multivibrator output pulse, i.e., the impact events count pulse, provide uniform input signals to the counting and data storage circuitries which follow. Such uniformity does not exist in the normally variant parameters of transducer signals.

Figure XII-12 is a schematic diagram of the signal-conditioning

circuitry of the curved-plate impact-detecting surfaces. This circuitry employs two amplifier channels, one for each of the two curved-plate detecting surfaces. Each amplifier channel has three stages of gain and a voltage-amplification capability of about 20,000:1. The outputs of the third stages of the two amplifier channels are applied to envelope detectors. The envelope detector outputs are combined by interconnection and are applied to the threshold selection circuit at the input of the high-sensitivity monostable multivibrator impact-event-counting pulse generator. In addition, this signal-conditioning circuitry has provision for a second lower sensitivity threshold of impact detection. The lower sensitivity threshold is determined by applying the transducer signal from the second stage of each amplifier channel to a second low-sensitivity envelope detector. The output sides of the secondary low-sensitivity envelope detectors are also combined by interconnection, and signals at this point are applied to a second low-sensitivity monostable multivibrator pulse-shaper circuit. If the signal amplitude from the low-sensitivity envelope detectors is sufficient at the input to the second multivibrator, both the low- and high-sensitivity multivibrators will be triggered and cycle. Thus, a dual, high- and low-sensitivity threshold capability exists in the curved-plate impact-detection system signal-conditioning circuitry. The low-sensitivity threshold of impact detection was set to about 1/100th of the high-sensitivity threshold.

Both signal-conditioning circuitry modules provide test points at amplifier output stages and multivibrator input stages for monitoring of calibration signals during flight-qualification testing. The power-supply input is filtered and each amplifier stage is decoupled. Each circuitry module is entirely enclosed within a copper case, which is single-point connected to the satellite's power-supply ground-reference point. Each unit consumes less than 25 milliwatts of power.

Impact-Event-Counting and Count-Storage Circuitries.- The output of the signal-conditioning circuitry of each threshold level of sensitivity of the impact-detection experiment was applied to impact-event-counting and count-storage circuitries. There were three independent counting and storage circuitries, one for each of the three impact-detection sensitivity-threshold levels. Each count-storage circuit had a capacity of 4,096 counts before recycling. As previously mentioned, details of the impact-event-counting and count-storage circuitries are found in chapter IV.

## SECTION IV - CALIBRATION

The calibration of the impact-detection experiments determined their response characteristics to impacts of known momenta. The average sensitivity of a detecting surface was determined by measuring its response to many impacts at various points on the surface. The appropriate correction to this average sensitivity was made by applying a correction factor derived from the restitution increment of the calibrating impact. Signal-conditioning-circuitry response to calibrating impacts was determined with respect to the varying supply voltages and circuitry temperatures anticipated in orbital flight.

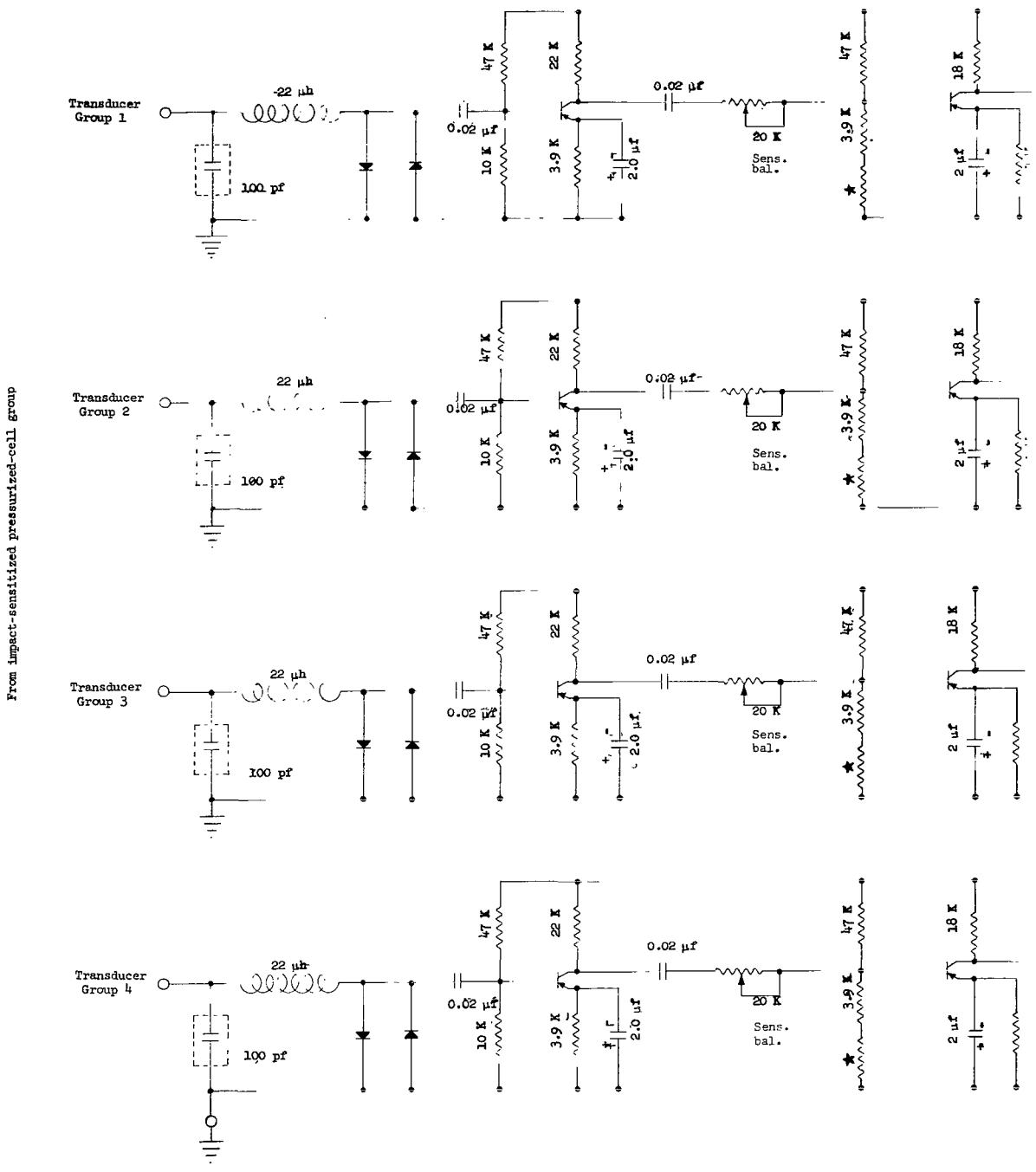


Figure XII-9.- Schematic diagram of signal-conditioning for impact sensitized pressurized cell.

starred resistance v

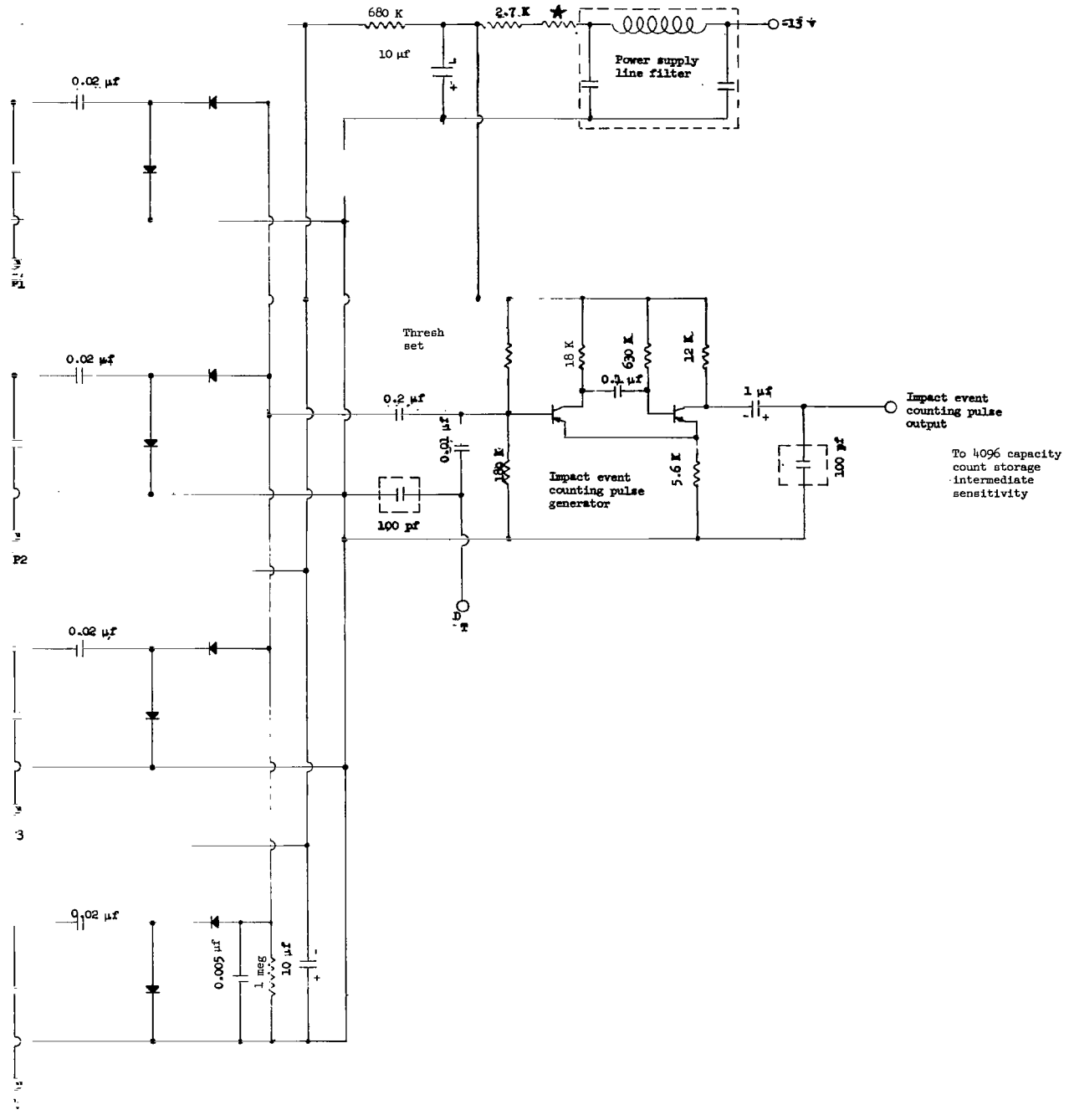


nsistors type 2N393; all diodes type 1N626; $T_{P1}$, $T_{P2}$, $T_{P3}$, $T_{P4}$, leads removed after testing;

lected during calibration.

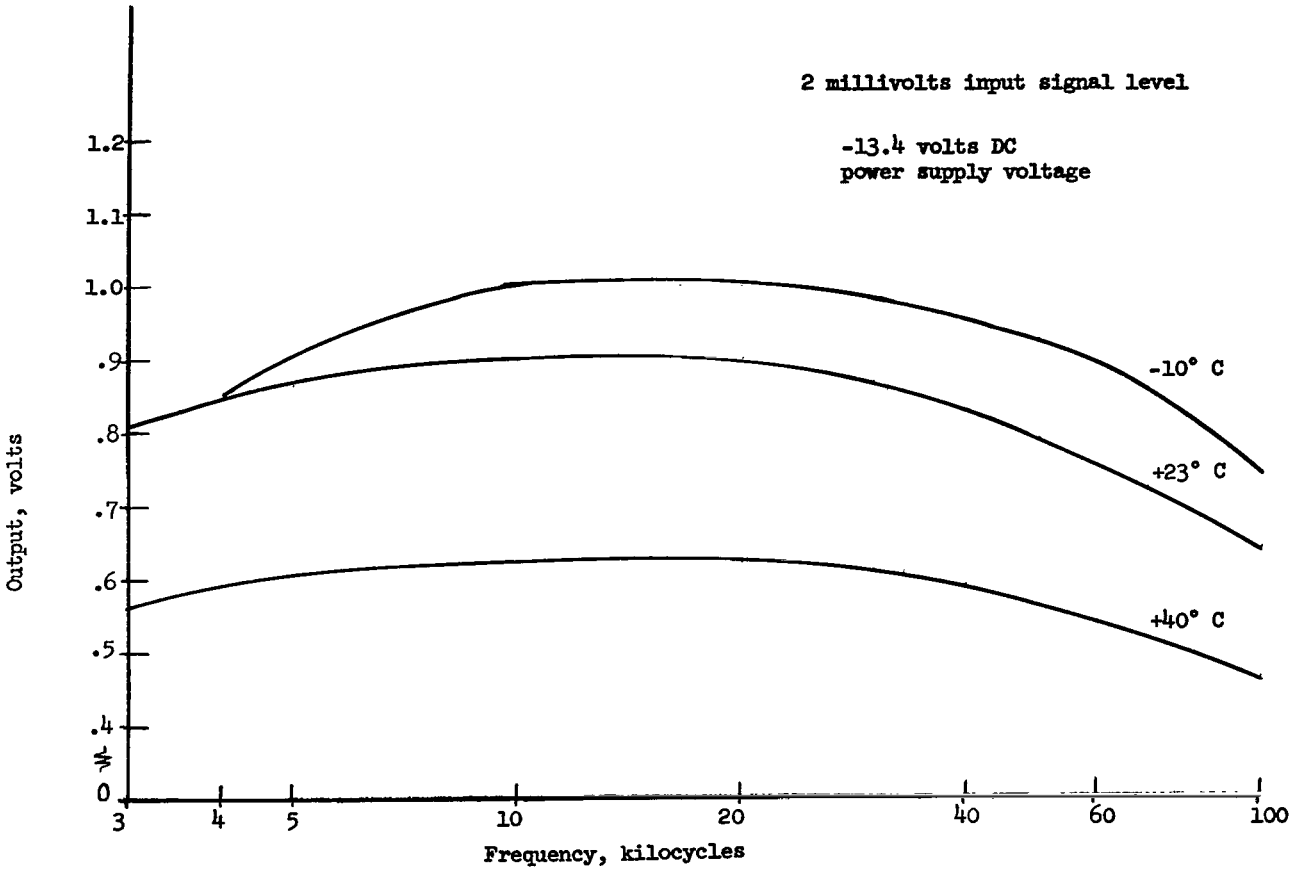


Figure XII-10.- Frequency-response characteristics of impact-sensitized pressurized-cell signal-conditioning circuitry.

The impact-calibration techniques employed particles of known mass falling upon detector surfaces through known heights, so that impact momenta were known. Linear response to impacting-particle momenta was assumed for this experiment. This assumption was in accordance with the practice of other United States experimenters performing similar experiments on satellites. The calibrating particles employed were spheres of aluminum oxide, of synthetic ruby and sapphire quality, ranging from 135 micrograms to 16.1 milligrams in mass. Dropping heights were accurately controlled, and were varied as required to obtain specific values of impact momenta. Drop heights were kept low, so that the effect of drag upon calculated momenta was negligible.

Figure XII-13 is a photograph of the manually operated calibrating mechanism employed in impact calibrations. The calibrating particles were positioned on the glass plate and gently pushed over its undercut beveled edge, designated by the arrow in the figure. The particles then fell through the known height onto the detecting surface positioned below. The manual-impact calibration technique produced consistently uniform transducer output provided the drop procedure was carefully controlled to minimize tangential and spin components of

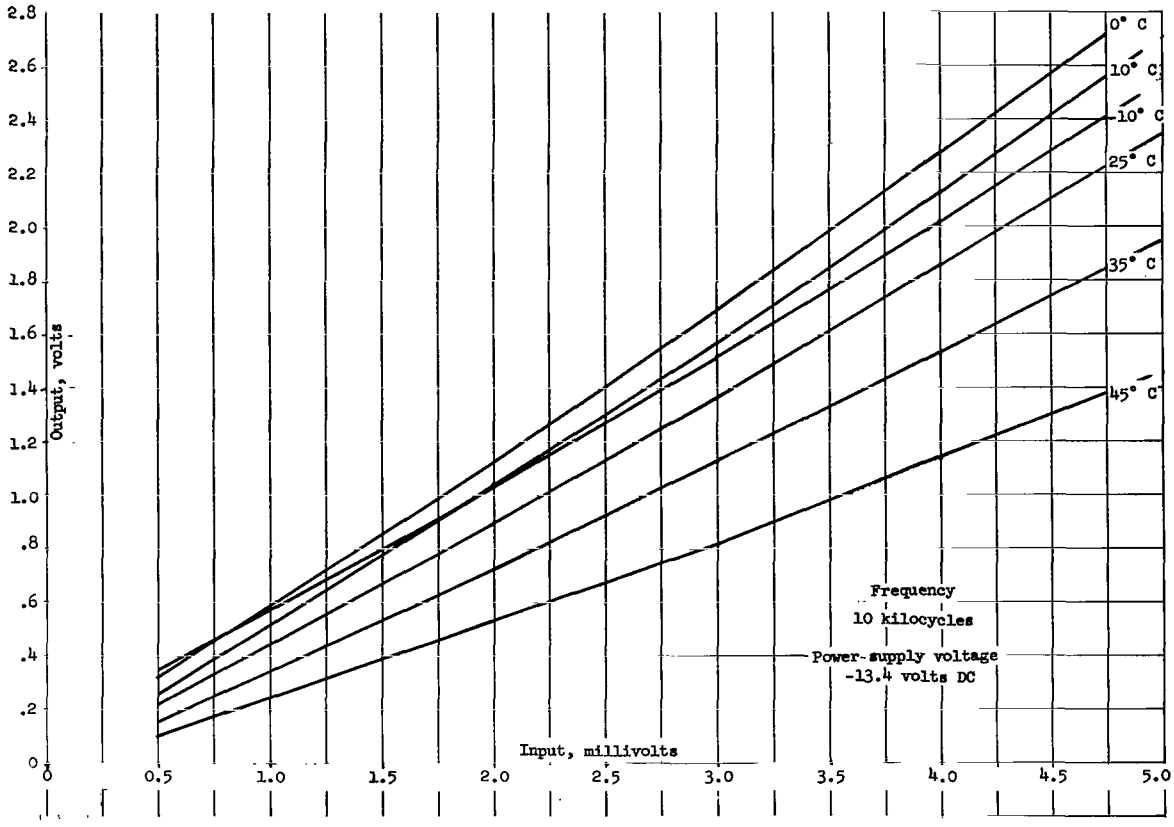


Figure XII-11.- Gain and linearity characteristics of impact-sensitized pressurized-cell signal-conditioning circuitry.

the impact-momentum vector. A very troublesome factor in the calibration of detecting surfaces was foreign matter in the path between the impact site and the piezoelectric element of the transducer assembly. Debris in this path produced unpredictable variations in transducer response to impact but was found to be avoidable by careful attention to cleanliness in both transducer assembly and calibration procedures.

A special test fixture was employed to measure the relative voltage sensitivities of the piezoelectric elements employed in transducer assemblies. The piezoelectric elements were then selected so that the electrically paralleled transducer assemblies in each transducer group were matched in impact sensitivity.

Special signal-conditioning circuitry was employed in the qualification and calibration of detector surfaces and transducers. The special circuitry was electrically identical to flight-model circuitries but provided additional test points for measuring impact-signal parameters and signal-conditioning-circuitry performance. The peak amplitude of the negative half of the amplified impact-signal envelope was monitored as the measure of the response of detecting surfaces and transducer assemblies to impact momenta.

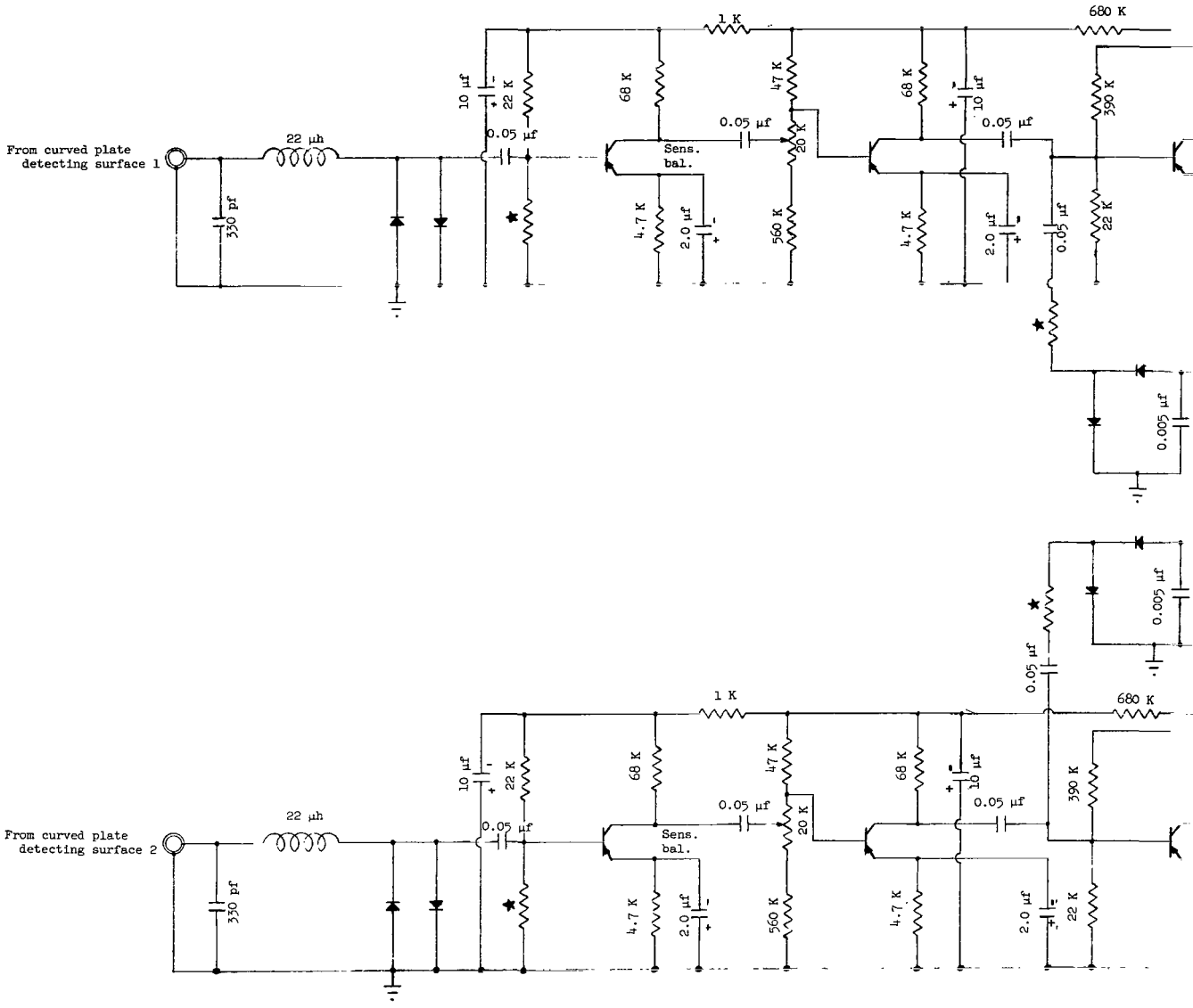


Figure XII-12.- Schematic diagram of signal-conditioning circuitry for curved-plate impact-detec

test point $H_T$ grounded after testing; sta

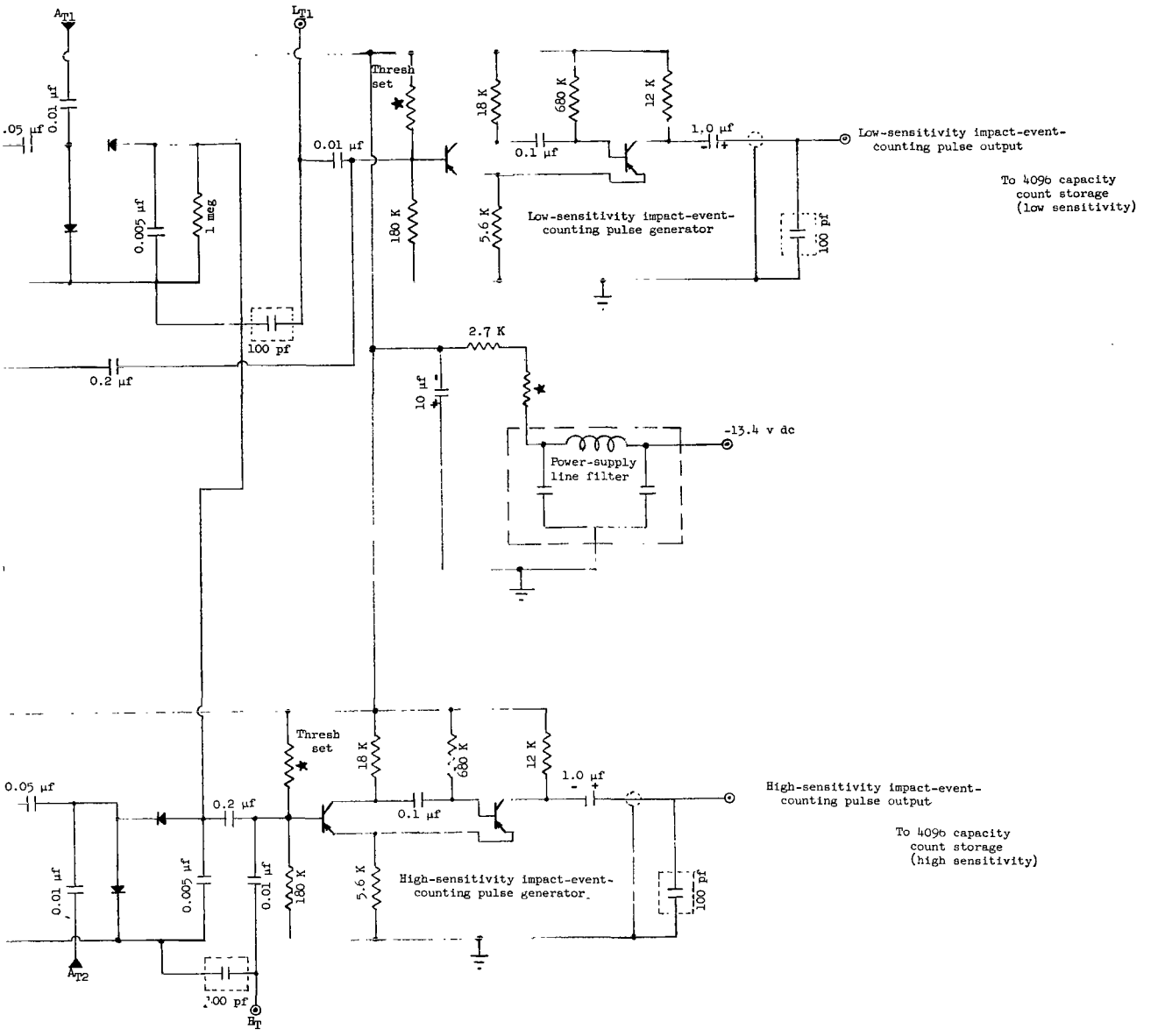


stem. All transistors type 2N393; all diodes type 1N626; $A_{T1}$ $A_{T2}$ leads removed after testing; sistance values selected during calibrations.

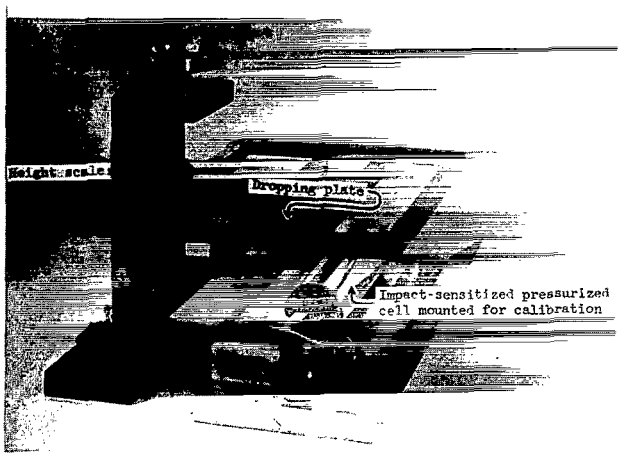


L-62-7320.1
Figure XII-13.- Manually operated impact-calibrating test fixture.

Figures XII-14 and XII-15 show the variation of response of the detecting surface of an impact sensitized pressurized cell with impact site and incidence angle. The impact response calibration of detecting surfaces such as that illustrated by this figure was determined by averaging many impacts at each impact calibrating site. Figure XII-16 shows the change of impact sensitized pressurized cell response variation caused by depressurization. The characteristics of figure XII-16 include the effects of atmospheric coupling and damping, although these effects would not be present in orbit. However, these factors were considered to be small in comparison with tolerances of other meteoroid impact-detection-system parameters.

Figure XII-17 shows the variation of impact response with impact site of a curved-plate detecting surface. The figure also shows the effects upon impact-response variation resulting from operating a pair of electrically paralleled transducer assemblies matched in impact sensitivity, and appropriately positioned on the detecting surface underside.

Since it has been assumed that the response of the impact-detection experiment is to the momentum of the impacting particle, the impact momenta of calibrating particles must be corrected for the restitution increment of the essentially elastic collision of a calibrating impact. Photographic measurement of rebound heights of many impacts was employed in determining the coefficients of restitution for the impact-detecting surfaces of the Explorer XIII.

The measurements of detecting-surface response and transducer-assembly response to calibrating impacts and signal-conditioning-circuitry performance under various conditions of temperature and voltage permit the definition of the impact-detection-system performance. Figures XII-18, XII-19, and XII-20 are the impact-sensitivity characteristics of the 0.01, 0.1, and 1.0 gram-centimeter per second momentum threshold impact-detection systems, respectively. The momentum thresholds are plotted against signal-conditioning-circuitry temperature at three power-supply voltages. The characteristics shown on the figures include the effect of the coefficient of restitution.

For the Explorer XIII impact-detection experiment, it has been assumed that the momentum response of the impact-detection systems which is observed in calibration procedures remains valid for meteoroid particle encounters, even though meteoroid-particle impact velocities are enormously greater, and masses correspondingly smaller, than calibrating-particle velocities and masses. The assumption that impacting meteoroids can be assigned an average impact velocity derived from observations of other meteoroid monitoring techiques, permits the

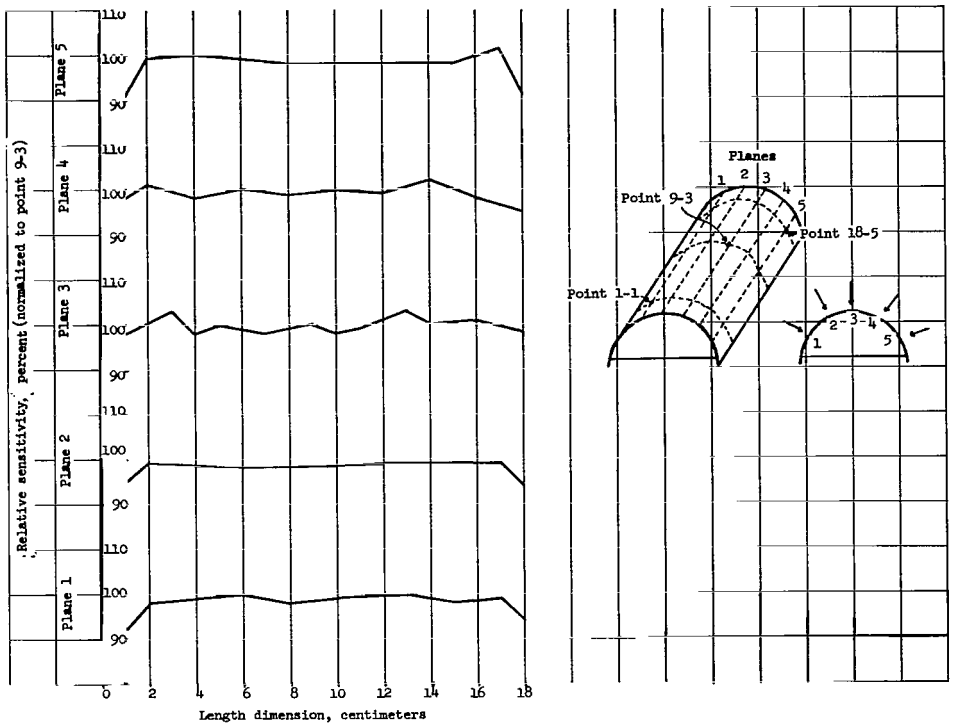


Figure XII-14.- Response variation of impact-sensitized pressurized cell with impact site.

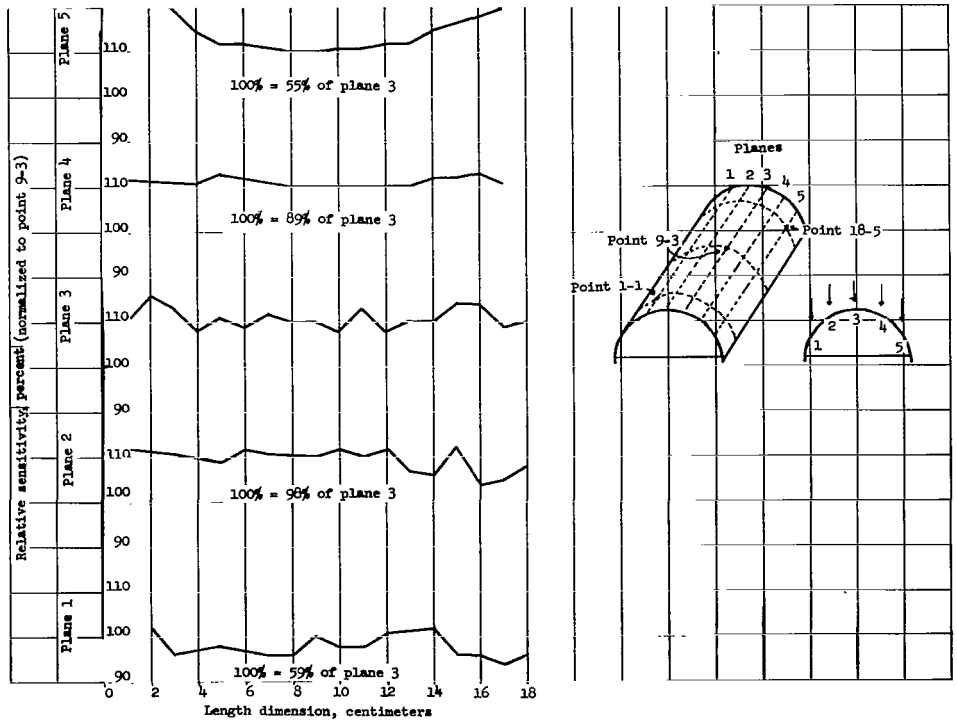


Figure XII-15.- Response variation of impact-sensitized pressurized cell with impact incidence angle.

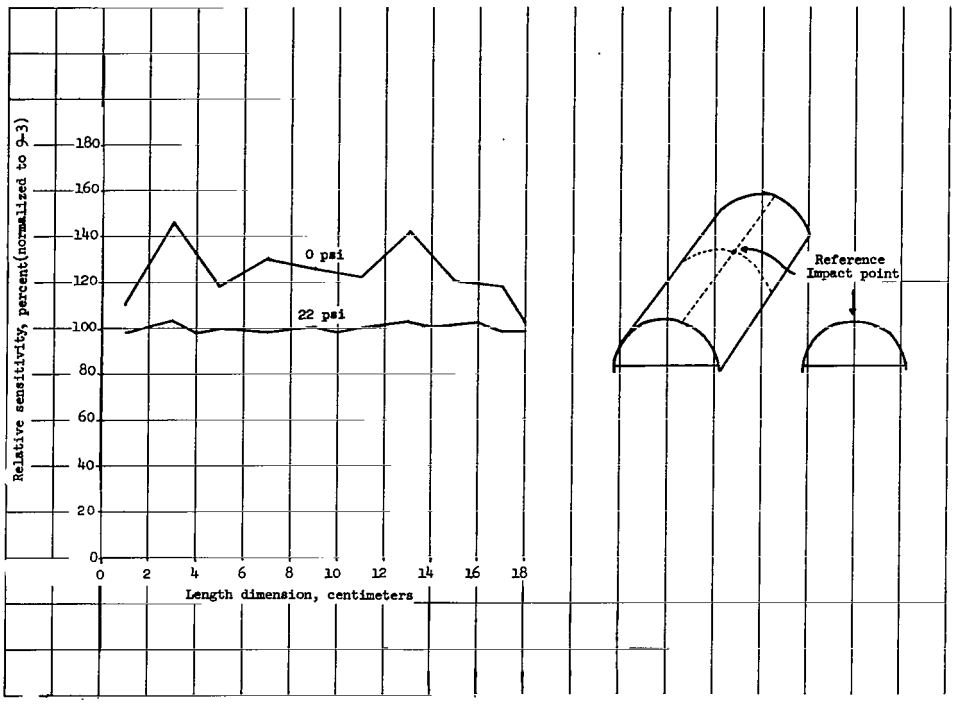


Figure XII-16.- Impact-sensitized pressurized-cell response variation with differential pressure.

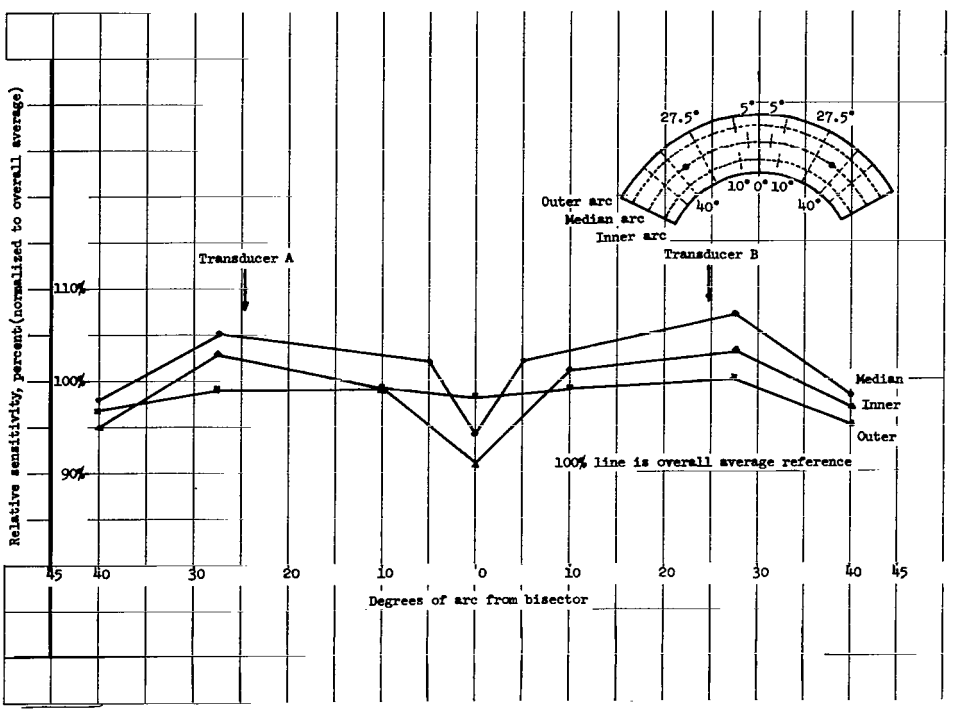


Figure XII-17.- Impact-response variation of curved-plate detecting surface with impact site.

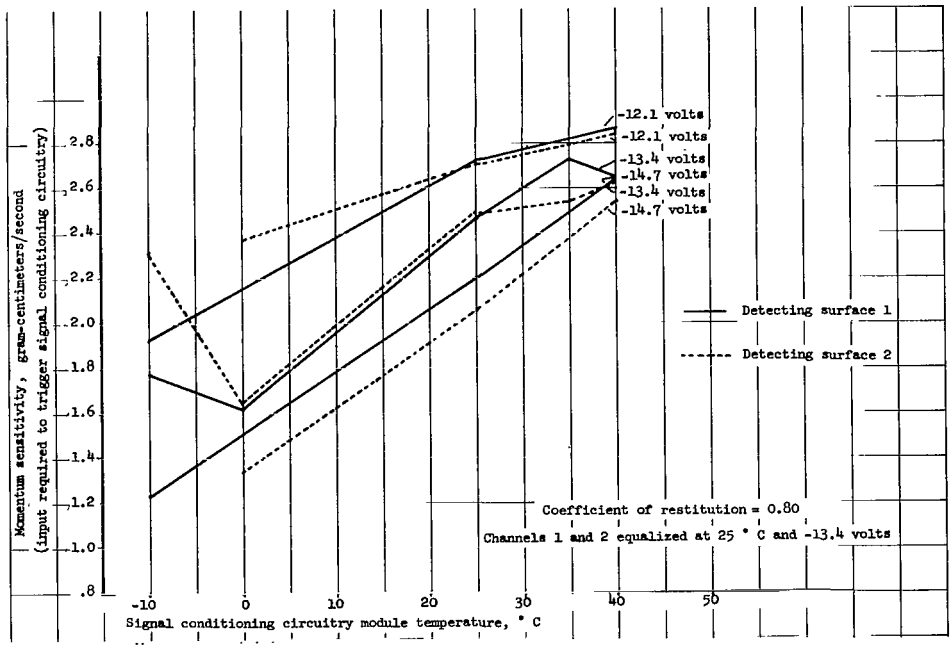


Figure XII-18.- Momentum-sensitivity threshold variation with signal-conditioning circuitry temperature and supply voltage for high-sensitivity curved-plate impact-detection system.

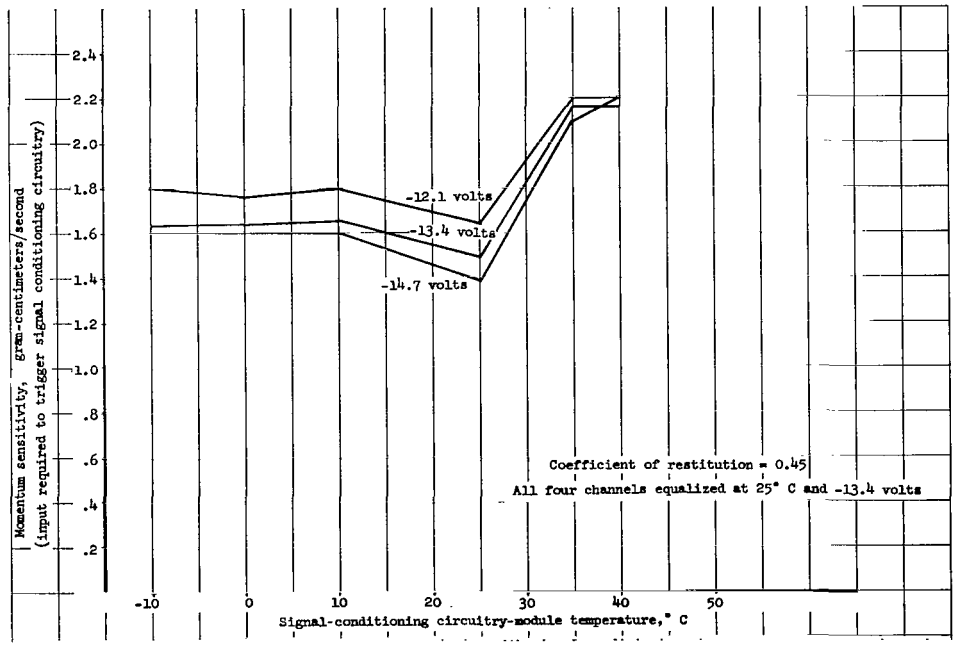


Figure XII-19.- Momentum-sensitivity threshold variation with signal-conditioning circuitry temperature and supply voltage for intermediate-sensitivity impact-sensitized pressurized-cell impact-detection system.

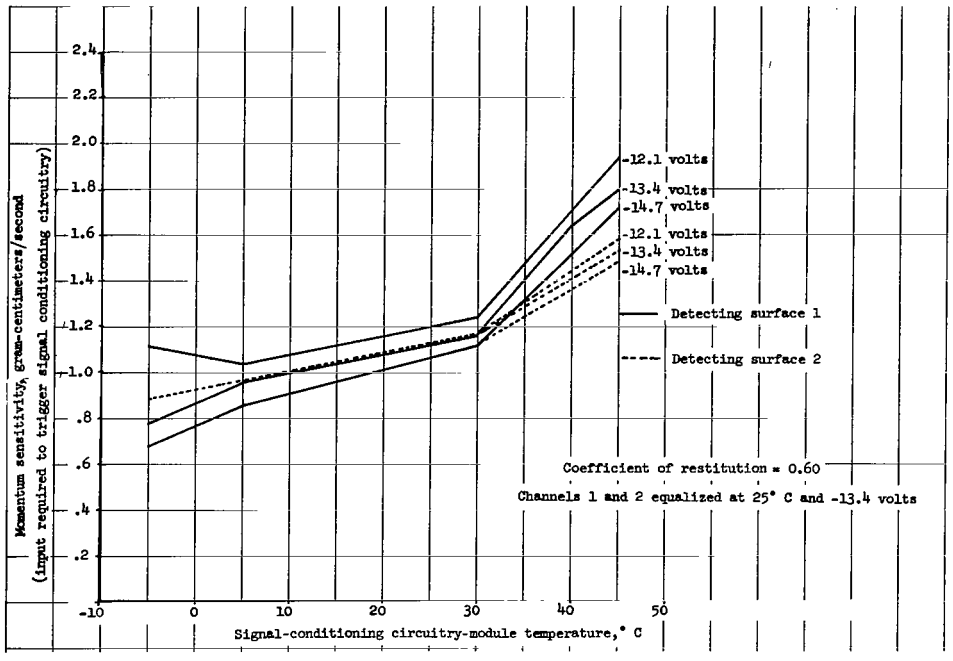


Figure XII-20.- Momentum-sensitivity threshold variation with signal-conditioning circuitry temperature and supply voltage for low-sensitivity curved-plate impact-detecting system.

assignation of an effective average-mass sensitivity threshold of the impact-detection systems. These two assumptions are in accordance with the practices of other United States experimenters (ref. 1).

Where the singularity of the Explorer XIII impact-detection systems precludes correlation with other similar experiments, as for example, in the case of the impact-sensitized detecting surfaces of the pressurized cells, an attempt has been made to provide sufficient calibration measurements so that the appropriate corrections can be applied when better knowledge of the proper way of doing so becomes available.

## SECTION V - RESULTS AND CONCLUSIONS

The meteoroid-impact-detection experiment of the Explorer XIII operated normally for the majority of its brief orbital lifetime. The actual values of the counts registered by each of the three momentum-sensing levels are listed in table XII-II. This table lists the accumulated count readout of telemetered data. Certain applicable corrections such as the modification of the effective area of detecting surfaces due to the earth shielding factor, and signal-conditioning-circuitry power-supply voltage and temperature fluctuations due to orbital flight would produce minor modifications appropriate to rigorous analyses of these data. Figure XII-21 illustrates summaries of the Explorer XIII

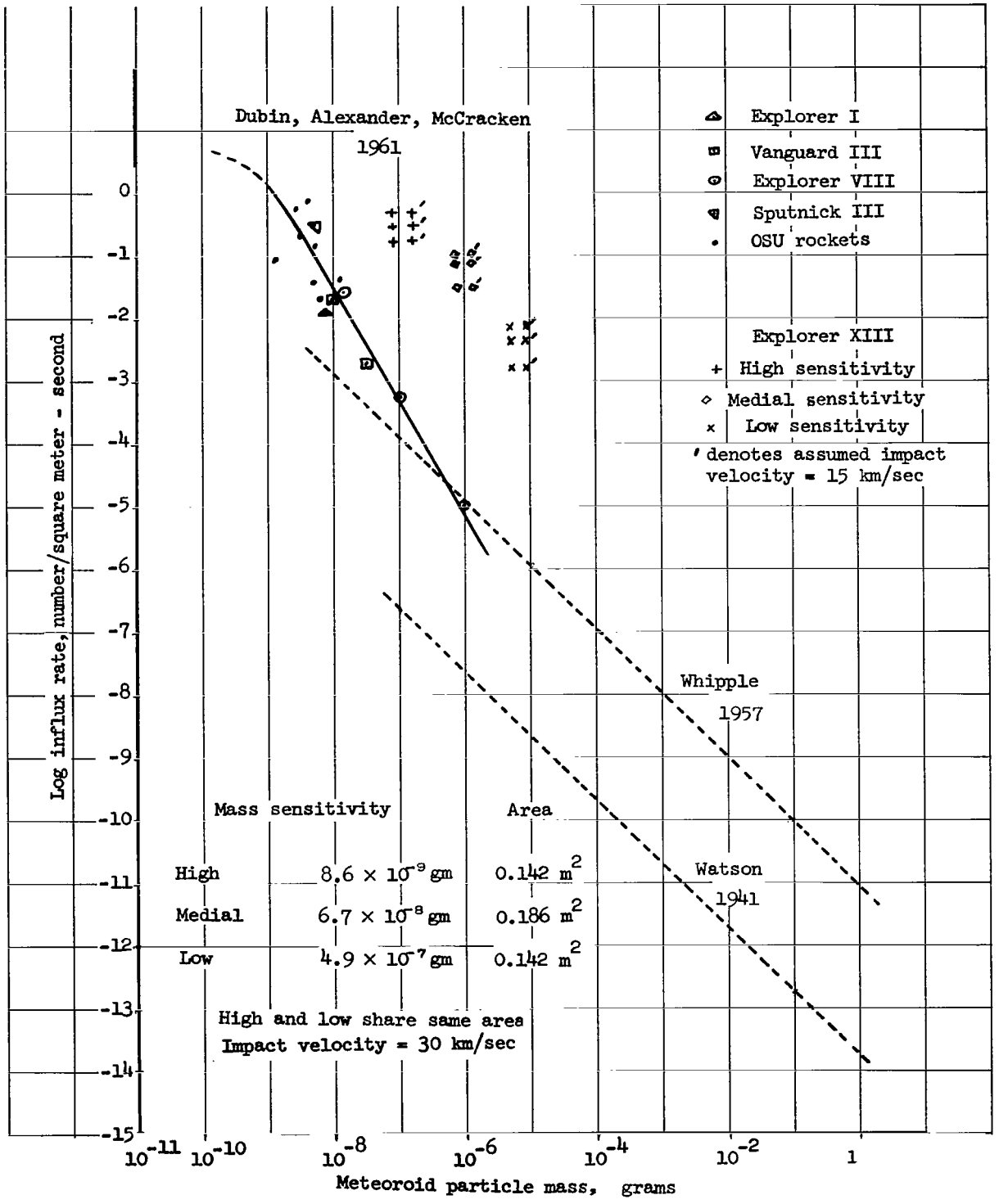


Figure XII-21.- Comparison of Explorer XIII impact-detection systems measured meteoroid influx with other meteoroid environment measurements. Vertical spread in Explorer XIII data points result from selecting orbital intervals; lower points are later intervals.

meteoroid-impact-detection-system counting rates of table XII-II compared with several models of the earth's meteoroid environment proposed by various observers. The figure shows that the measured impact flux rates are substantially higher than those measured by other similar satellite experiments represented by the curve of Dubin, Alexander, and McCracken, from reference 1, although these rates were decreasing with the satellite's time in orbit. No explanation is known for this circumstance, and better definition of the Explorer XIII meteoroid environment cannot be realized because of the lack of data.

It is possible that the orbit of Explorer XIII could have been a factor in producing the high counting rates of the meteoroid-impact-detecting systems. As has been described in previous sections of this compilation, the orbit had very low initial perigee (113.5 kilometers) which subsequently lowered progressively. Aerodynamic mechanical perturbances and temperature effects on the impact-sensing transducer elements might have caused the impact-detecting systems to register signals which were not meteoroid impacts.

Considering these factors, the meteoroid-impact data gathered by the flight of the Explorer XIII must be considered inconclusive. However, it is significant to point out that a valid experimental technique has been developed for the meteoroid hazard research satellite series. Indications are that more significant results would have been obtained from this experiment had the satellite remained aloft and performed satisfactorily for a longer period of time.

## SECTION VI - REFERENCE

XII-1 McCracken, C. W., Alexander, W. M., and Dubin, M.: Direct Measurements of Interplanetary Dust Particles in the Vicinity of Earth. NASA TN D-1174, 1961.

TABLE XII-I.- CHARACTERISTICS OF THE IMPACT DETECTING SURFACES

| Shape | Size, cm | Weight, gm | Area, $cm^2$ | Material | Coating |
|---|---|---|---|---|---|
| Forward shell curved plates (2) | | | | | |
| Conical section | 12.5 width<br>59.2 outer circumference<br>32.8 inner circumference<br>0.079 thickness | 430 ± 10 | 709 (each)<br>1418 (total) | 410 stainless steel | Sandblasted surface; oxidized |
| Pressurized cells (20) | | | | | |
| Semi-cylindrical | 18.8 length<br>4.93 diameter<br>0.0125 thickness | Part of pressurized-cell weight | 92.8 (each)(projected)<br>1856 (total) | Beryllium-copper | Deposited aluminum surcoated with silicon monoxide |

TABLE XII-II.- EXPLORER XIII METEOROID IMPACT DETECTION EXPERIMENT COUNT ACCUMULATION

| Orbit | Minitrack recording station | Date/Time (Greenwich Mean Time) | Elapsed time from injection | Impact experiment count accumulation sensitivity threshold, gm-cm/sec | | |
|---|---|---|---|---|---|---|
| | | | | Low | Intermediate | High |
| Injection | | 25/1839 | 0 | --- | ---- | ---- |
| 1 | Blossom Point | 25/2011 | 92 | 0 | ---- | ---- |
| | Grand Forks | 25/2011 | 92 | 0 | ---- | ---- |
| 9 | Antofagasta | 26/1002 | 923 | 124 | ---- | ---- |
| 10 | Quito | 26/1146 | 1027 | 132 | ---- | ---- |
| 13 | Fort Myers | 26/1513 | 1234 | 153 | 0 | 0 |
| | Blossom Point | 26/1515 | 1236 | 153 | 0 | 0 |
| 14 | Blossom Point | 26/1658 | 1339 | 156 | 157 | 538 |
| 15 | Fort Myers | 26/1840 | 1441 | 156 | 258 | 2400 |
| 21 | Santiago | 27/0445 | 2046 | 166 | 1425 | 3957 |
| 22 | Santiago | 27/0621 | 2141 | 171 | 1476 | 4214 |
| 23 | Antofagasta | 27/0803 | 2244 | 171 | 1506 | 4403 |
| 28 | Woomera | 27/1542 | 2699 | 172 | ---- | ---- |

*"The aeronautical and space activities of the United States shall be conducted so as to contribute . . . to the expansion of human knowledge of phenomena in the atmosphere and space. The Administration shall provide for the widest practicable and appropriate dissemination of information concerning its activities and the results thereof."*

—NATIONAL AERONAUTICS AND SPACE ACT OF 1958

# NASA SCIENTIFIC AND TECHNICAL PUBLICATIONS

TECHNICAL REPORTS: Scientific and technical information considered important, complete, and a lasting contribution to existing knowledge.

TECHNICAL NOTES: Information less broad in scope but nevertheless of importance as a contribution to existing knowledge.

TECHNICAL MEMORANDUMS: Information receiving limited distribution because of preliminary data, security classification, or other reasons.

CONTRACTOR REPORTS: Technical information generated in connection with a NASA contract or grant and released under NASA auspices.

TECHNICAL TRANSLATIONS: Information published in a foreign language considered to merit NASA distribution in English.

TECHNICAL REPRINTS: Information derived from NASA activities and initially published in the form of journal articles.

SPECIAL PUBLICATIONS: Information derived from or of value to NASA activities but not necessarily reporting the results of individual NASA-programmed scientific efforts. Publications include conference proceedings, monographs, data compilations, handbooks, sourcebooks, and special bibliographies.

***Details on the availability of these publications may be obtained from:***

SCIENTIFIC AND TECHNICAL INFORMATION DIVISION

NATIONAL AERONAUTICS AND SPACE ADMINISTRATION

Washington, D.C. 20546